Nontraditional Methods of Sensing Stress, Strain, and Damage in Materials and Structures

Second Volume

George F. Lucas
Peter C. McKeighan
Joy S. Ransom

Editors

ASTM STP 1323

Lucas • McKeighan • Ransom
Nontraditional Methods of Sensing Stress, Strain, and Damage in Materials and Structures
STP 1323

STP 1323

Nontraditional Methods of Sensing Stress, Strain, and Damage in Materials and Structures: Second Volume

G. F. Lucas, P. C. McKeighan and J. S. Ransom, editors

ASTM Stock Number: STP1323

ASTM
100 Barr Harbor Drive
PO Box C700
West Conshohocken, PA 19428-2959

Printed in the U.S.A.

Photocopy Rights

Peer Review Policy

Each paper published in this volume was evaluated by two peer reviewers and at least one editor. The authors addressed all of the reviewers' comments to the satisfaction of both the technical editor(s) and the ASTM Committee on Publications.

To make technical information available as quickly as possible, the peer-reviewed papers in this publication were prepared "camera-ready" as submitted by the authors.

The quality of the papers in this publication reflects not only the obvious efforts of the authors and the technical editor(s), but also the work of the peer reviewers. In keeping with long-standing publication practices, ASTM maintains the anonymity of the peer reviewers. The ASTM Committee on Publications acknowledges with appreciation their dedication and contribution of time and effort on behalf of ASTM.

Printed in Saline, MI
April 2001

Foreword

This publication, Nontraditional Methods of Sensing Stress, Strain, and Damage in Materials and Structures: Second Volume, contains papers presented at the symposium of the same name held in Kansas City, Missouri, on 17 November 1999. The symposium was sponsored by ASTM Committee E8 on Fatigue and Fracture. The symposium co-chairpersons were George F. Lucas, MTS Systems Corporation, Peter C. McKeighan, Southwest Research Institute, and Joy S. Ransom, Fatigue Technology Incorporated.

Overview

A mechanical test is of little value without some type of sensor to (a) control the test, (b) provide a measurement of physical behavior or (c) indicate when the test is completed. The most common sensors are those that measure force, displacement and strain. Although many sub-classifications of these devices exist, industrial development of new force, displacement and strain sensors is ongoing, often driven by a new application where the parameters exceed the limits of the currently available sensors. Perhaps a good parallel example of this is the ceramics development that occurred during research concerned with the now defunct high-speed civil transport. Had this aircraft not been envisioned, several of the current high temperature materials would likely not exist.

The focus of this symposium is the development and application of nontraditional sensors. For instance, several novel methods to measure strain in a body are available using non-contacting techniques. In particular, there has been a large amount of work using vision-based sensors to measure the deformation field on a material or structure. Although this is only one example, there are other new, novel methods of measuring parameters that may directly correlate with some form of damage within the material or structure. The purpose of this symposium is to assess the state of the art of these sensing methods and examine their future potential use as standardized tools within the testing communities. Encouraging use of these new sensing methods and extending them into industrial application will presumably be a consequence of the symposium.

This symposium, held in November of 1999 in Kansas City, is the second in a series of symposia concerned with nontraditional methods of sensing stress, strain and damage. The first, STP 1318, was held in May of 1996 in Orlando, Florida and was preceded by two workshops on the same topic in earlier years. These Symposia and Proceeding Workshops were instigated by task group E08.03.03 on Sensors, which is a task group of the committee on Fatigue and Fracture and its subcommittee on Advanced Apparatus. The scope of this task group is to develop standards and encourage technology interchange concerning measurement sensors that are used in determining fatigue and fracture characteristics of materials and structures.

Perhaps one of the major differences between the first and second symposium (a span of three and a half years) was the increase in capability apparent in personal computers. A close examination of all of the papers in this symposium will show that at the heart of all of the systems presented was a computer. As we all know, the speed of the CPU's has been doubling every two years to eighteen months (Moore's Law). However what became apparent during the symposium was not the pivotal role that increased processing speed was playing but rather the enormous impact of infinitely available, low cost RAM and storage space. This is probably most clearly evident for vision-based sensors that manipulate and interpret images. Greater RAM allowed more on-the-fly computations and high-speed storage space (gigabytes plus) implying enhanced flexibility.

The twelve papers included in this STP are very diverse, both from the viewpoint of the applications considered as well as concerning the sensors applied. Four of the papers included in this STP utilize imaging systems to infer deformation fields. Helm, Sutton and Boone use their 3-D system to characterize fatigue crack growth for aluminum panels under tension-torsion loading. Towse *et al.* describe a general purpose, 2-D non-contacting extensometer derived from video images and capable of tracking multiple targets at high speed. Two other

papers, Smith and Bay and Nicollela *et al.* examine strain fields in biological material (bone) using image correlation techniques.

Two papers focused primarily on acoustic emission techniques: McKeighan *et al.* examined crack nucleation and growth from defects in titanium and Ma and Takemoto considered thermal fracture in coatings subjected to cyclic laser irradiation. Two other papers focused on fiber optic methods of measuring strain and deformation. Chen and Sirkis examined the costs and benefits of fiber optic versus conventional electric strain gages. Conversely Tu *et al.* measured long-term creep deformation using quartz optical fiber marking, remote monitoring and image processing.

The remaining four papers examined relatively unique applications and sensors. Suhling and Jaeger present work where the structural reliability of IC chips is measured using piezoresistive sensors bonded to the chip substrate. Morimoto and Fujigaki present work concerning the real-time phase analysis of Moire images to analyze shape, strain and stress. The final two papers concern damage measurement. Ranganathan *et al.* examines methods for quantitative fractography where the fracture surface of a failed specimen can be used to assess loading conditions that led to failure. Finally, Burkhardt and Crouch present a magnetic nonlinear harmonics approach to detect localized plastic deformation in pipelines.

Organizing these papers in some cogent manner is a challenge in view of the diversity of applications, methods, sensors and focus. Nevertheless, the approach adopted is intended to address the focus of the papers. In the first section, *Fracture Mechanics and Structural Integrity,* the papers that talk about cracks (either crack growth or fracture) or general stress-strain behavior are included. The papers that address the damage state of a material are included in the section entitled *Damage Evolution and Measurement* whereas the final section considers *Strain and Displacement Measurement Techniques.*

Following the symposium, a brief panel discussion was held focussing on issues such as where sensor development was going, what was spurring sensor development and what ASTM standardization activities could assist this process. This was a lively discussion and it is succinctly summarized at the conclusion of this book after all of the technical papers. The technical community is clearly faced by some technical challenges—first and foremost being the cost of new sensors and the magnitude of the effort required to develop them. ASTM can play an important role in this process by insuring that the standards are available to assess the performance of sensors once developed. However the breadth of the standards required for this and covering sensor technology not yet even discovered is awe inspiring.

The editors would like to express their sincere appreciation to all of the authors and co-authors responsible for the papers included in this STP and the presentations made during the symposium. Furthermore we would like to recognize the efforts of the reviewers whose high degree of professionalism and timely response ensures the quality of this publication. Finally, the editors would also like to express their sincere gratitude to ASTM planning and editorial staff for their assistance with the symposium as well as their critical input to this special technical publication.

Finally, it should be noted that Tait S. Smith, co-author of the paper "Experimental Measurement of Strains using Digital Volume Correlation" formerly with the University of California, Davis, received the "Best Presented Paper Award" for his excellent presentation at the symposium. This honor was bestowed based upon the critiques of five seasoned professionals in the audience.

Peter C. McKeighan
Southwest Research Institute
San Antonio, TX
Symposium co-chairman and editor

Contents

Fracture Mechanics and Structural Integrity

J. D. Helm,[1] M. A. Sutton,[2] and M. L. Boone[2]

Characterizing Crack Growth in Thin Aluminum Panels Under Tension-Torsion Loading Using Three-Dimensional Digital Image Correlation

---

Reference: Helm, J. D., Sutton, M. A. and Boone, M. L., **"Characterizing Crack Growth in Thin Aluminum Panels Under Tension-Torsion Loading Using Three-Dimensional Digital Image Correlation,"** *Nontraditional Methods of Sensing Stress, Strain, and Damage in Materials and Structures: Second Volume, ASTM STP 1323,* G. F. Lucas, P. C. McKeighan, and J. S. Ransom, Eds., American Society for Testing and Materials, West Conshohocken, Pa, 2001.

Abstract: The enclosed work was performed to determine whether a critical crack opening displacement (COD) criterion can be used to predict the stable crack growth behavior of thin, 2024-T3 aluminum fracture specimens experiencing tension and torsion loading. Due to the complexity of the large deformations that occur near the crack tip in a single edge-cracked specimen under torsion loading, a state of the art three-dimensional computer vision system was developed and employed to make the three-dimensional vector displacement measurements required to determine COD. Results from the experimental program indicate that the three-dimensional surface profile and deformation measurement system was fully capable of making the required measurements, even in the presence of large, out-of-plane displacements and surface strains that occurred during the tension-torsion loading process. Specifically, the measurements show that (a) critical COD for tension-torsion loading is constant during crack growth, (b) COD is approximately 8% larger than observed for in-plane tension-shear and (c) the surface strain fields during crack growth are quite complex due to the coupling of out-of-plane displacements and in-plane surface strains.

Keywords: mixed mode fracture experiments; tension-torsion loading; three-dimensional digital image correlation; non-contacting measurements; crack opening displacement

---

[1]Chief Engineer, Correlated Solutions, Inc.; 300 Main Street; Suite C113-N; Columbia, SC 29208

[2]Professor and former graduate student, respectively; Department of Mechanical Engineering; University of South Carolina; Columbia, SC 29208

INTRODUCTION

Recent mixed-mode I/II fracture experiments *[1-4]* and theoretical developments *[5,6]* indicate that two-dimensional COD is a robust fracture parameter that can be used to accurately predict the onset and direction of stable crack growth. Here, two-dimensional COD is defined as

$$COD_{2D} = [\,(\Delta u)^2 + (\Delta v)^2\,]^{1/2} \qquad (1)$$

where the relative displacement components, Δu and Δv, in the x-direction (along original crack direction) and y-direction (perpendicular to crack), respectively, are computed at a specific distance behind the current crack tip by the equations;

$$\Delta u = u^{above} - u^{below}$$
$$\Delta v = v^{above} - v^{below} \qquad (2)$$

where u^{above} (v^{above}) and u^{below} (v^{below}) are the displacements in the x-direction (y-direction) for points located above and below the existing crack line, respectively, at a fixed distance behind the current crack tip. In this work, and in previous work, the authors selected the distance behind the crack tip to be 1mm.

It is well known that flaws growing in aerospace structures oftentimes are subjected to a combination of mixed mode I/II/III conditions. In thin fuselage material, these complex crack tip conditions are due to local, out-of-plane motion *[7]* of the unconstrained cracked surfaces. The out-of-plane deformation will occur under either internal pressure or tensile loading *[8]*.

To develop a better, physical understanding of the crack growth processes that occur under mixed mode loading, as well as provide a quantitative set of measurements for use in model verification, a series of tension-torsion *[9,10]* laboratory-scale experiments using thin sheet, 2024-T3 aluminum specimens have been performed. During these experiments, the crack tip opening displacement data was acquired using a state-of-the-art, three-dimensional computer vision system. In the following sections, the test specimen is presented along with the experimental procedures used to perform the experiments. Next, a brief summary of the three-dimensional computer vision method is given. Then, results from a series of tension-torsion experiments are presented, including (a) the first known three-dimensional COD data and (b) typical strain fields acquired just prior to stable crack growth. Finally, a short discussion of the results is presented.

TENSION-TORSION SPECIMEN AND TEST CONFIGURATION

Figure 1 presents a schematic of typical tension-torsion specimen geometry. The 2.3 mm thick specimens were machined from unclad 2024-T3 aluminum and fatigue pre-cracked under tensile loading in the L-T orientation so that the initial crack length to width ratio is a/w = 0.0833. All tests were performed on a 50K MTS test frame using an MTS Testar system with PID controller and user-

generated control programs. To perform each experiment, the following control system process was employed. Axial displacement was used to control load application to the specimen. During the loading process, axial load cell output

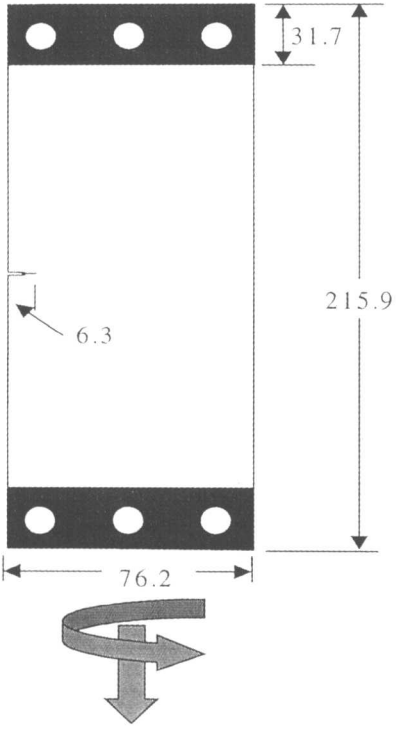

Figure 1: Tension-torsion specimen (units in mm)

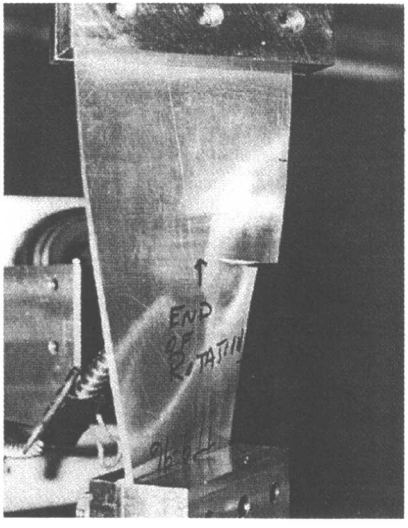

Figure 2: Large deformations during loading of tension torsion specimen

was input to the torsion actuator to generate a proportional, applied torque. Finally, the torsion rotation was increased until the required torque was attained. Since three channels of input are used to control the test process, it is necessary to set appropriate tuning factors for all three channels of input to ensure stability of the system for the type of specimen being tested. It is noted that the control process described above was slightly unstable at low levels of applied loading; for loads greater than 400 N, the system was unconditionally stable.

Defining stress components on a rectangular cross-section by $S_T = 3T(t^2\, w)^{-1}$ and $S_P = P(t\, w)^{-1}$, where t is the specimen thickness and w is the specimen width, experiments were performed at five levels of S_T/S_P in the range $0.0 \leq S_T/S_P \leq 6.64$. In this work, COD results are reported for S_T/S_P = 0, 1.66, 3.32, 4.98 and 6.64. Additional results, such as crack surface profiles and strain fields, are reported for S_T/S_P = 0.00, 3.32.

OVERVIEW OF THREE-DIMENSIONAL DEFORMATION MEASUREMENT PROCESS

Figure 2 graphically illustrates the large deformations that occur prior to and during stable crack extension as the rectangular specimen is quasi-statically loaded in tension and torsion; fatigue pre-cracking did not result in large specimen deformations. To measure the *three-dimensional vector displacements* for points on the specimen surface in Fig. 2, a unique digital image correlation system (DIC-3D) was developed specifically for this experiment. The DIC-3D system is capable of measuring the full, three-dimensional surface displacement field for a structure deforming in three-dimensions *[8,9]*, including the presence of large in-plane and out-of-plane rotations, large displacements and large strains.

To make accurate displacement and shape measurements with a 3-D vision system, both (a) high quality calibration of the system and (b) a matching process that accounts for both lens and perspective effects when determining the optimal deformation parameters are required. Figure 3 shows a typical 3-D vision system.

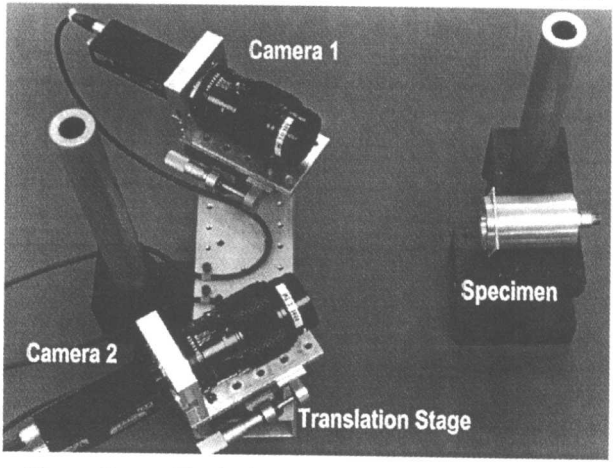

Figure 3: Typical system for three-dimensional displacement measurements.

In our work, the camera and lens systems are modeled as a pinhole device with a correction to account for Seidel lens distortion *[9-11]*.

The pinhole camera projection equations that govern the use of these cameras typically require that the imaging characteristics of a camera are modeled by five parameters. In this work, the parameters are (1) pinhole distance (phd), (2,3) location of the center of the image (C_x, C_y), (4) lens distortion parameter, κ, for Seidel correction and (5) the aspect ratio, λ, of the sensors. In addition to these parameters, six parameters (X_o, Y_o, Z_o, and α, β, γ) are required to describe the relationship between a camera and the coordinate system of the calibration grid. Here, (X_o,Y_o,Z_o) describe the position in space of the grid relative to the camera and (α,β,γ) describe the angular orientation of the grid relative to the camera.

Calibration of the two-camera computer vision systems determines the relative position and orientation of the camera relative to the grid, as well as the operating characteristics of both cameras. The calibration system is based on a series of images of a grid with known line spacing *[10, 11]*. Each camera is

calibrated to the grid individually. Since the positions of both cameras are known relative to the same grid, their relative orientation and position are also known. To calibrate each camera in the stereo-vision system, an image of the grid is taken. The camera is then moved perpendicular to its sensor plane and a second image is taken. Non-linear optimization is used to obtain the parameters that best describe the position and operating characteristics of the camera. The process is then repeated, without moving the grid, for the second camera. Verification tests are discussed in detail in Reference *[11]*.

Once calibration is completed, the stereo vision system can be used to measure both the shape of the object surface (profiling) and also the full field, three-dimensional displacement measurements. Similar to two-dimensional image correlation, the three-dimensional measurement system uses a random pattern bonded to the surface to provide a unique set of features to map image locations from one camera to the other. Software, designated DIC-3D, has been written to perform the process of optimal matching of subsets in both cameras to locate the position and orientation of this region on the object. The analysis uses two pairs of images taken of the surface of the object by camera one and camera two, with each pair of images acquired at the same time. The two pairs of images are used to obtain the three-dimensional surface displacement field by employing a small square section of the image taken by camera one before deformation as the "reference" image. Using a "projection with back-projection" process developed by the authors, both the initial position of the subset on the object (e.g., the surface profile) and the three-dimensional surface displacement of the same subset due to deformation can be measured.

Cross-correlation is used to establish an error measure and obtain the best match of the reference gray level pattern to corresponding patterns in each of the images. The error function is optimized to determine the initial position and displacement of a specific subset on the surface of the object. By continuing the analysis on other portions of the image in camera one, both the full-field profile and the full-field, three-dimensional displacements of the surface of the object for the entire field of view shared by both cameras are measured. A complete explanation of the 3D image analysis process is given in *[11]*.

THREE-DIMENSIONAL COMPUTER VISION SYSTEM FOR COD AND SURFACE STRAIN MEASUREMENTS FOR TENSION-TORSION SPECIMEN

Conceptually, COD should be measured sufficiently close to the crack tip to reflect the crack tip deformations that result in crack tip damage and crack extension. Since the specimen surfaces are expected to undergo three-dimensional displacements, a generalized definition for three-dimensional crack opening displacement (COD) is given in the following equation

$$\mathbf{COD} = [\,(\Delta u)^2 + (\Delta v)^2 + (\Delta w)^2\,]^{1/2} \qquad (3)$$

where the additional relative displacement component, Δw, is perpendicular to the original specimen surface and is measured at the same distance behind the current crack tip as are Δu and Δv in (2) and is given by the equation;

$$\Delta w = w^{above} - w^{below} \tag{4}$$

Following procedures outlined previously *[1-6]*, COD was measured at 1 mm behind the current crack tip in this work. To quantify COD accurately in this region behind the current crack tip, the DIC-3D system was used to image a region approximately 4mm by 4mm in size. Due to both the high magnification required and the need to follow the moving crack tip, special considerations were used when setting up the two-camera system. These considerations included (a) camera mounting, (b) system stability and (c) crack-tip tracking.

The camera mounts used for these tests were specially designed to reduce any motion of the camera and lenses by incorporating the mount into the C-mount to Canon lens adapter, while providing full support for the lens system. Special care was used to align the camera mounts with the translation stages. To obtain camera translation that was perpendicular to the sensor plane, both camera mounts were adjusted (using thin shims) until the translation of the camera produced a displacement field indicating a nearly pure radial dilation of the image.

To achieve overall stability in the vision system, the cameras were attached to an extruded aluminum cross bar. The honeycomb construction of the cross bar created a lightweight, yet rigid, support member for the camera system. In addition to the rigid cross bar, the connecting mount securing the cross bar to the calibration fixture and to the translation stage was re-designed to minimize any bending forces produced when clamping the system to the holding fixtures.

To track the crack tip region during stable crack extension, the vision system was mounted on a four-axis translation/rotation system. The system was capable of translating in all three directions, as well as rotating about a vertical axis to adjust for torsion/twisting of the specimen. Moving and rotating the entire system maintained a focused view of the crack tip area throughout the crack extension process.

Finally, translation tests were performed to assess the accuracy of the system. For our tension-torsion experimental setup, calibration and translation tests indicate that the standard deviation error in each displacement component was +/- 1 μm. This error estimate was obtained by fitting a least square constant vector displacement to the measured data for each translation test. It is worth noting that conversion of displacement errors to strain error estimates is difficult due to the dependence of strain errors on (a) the form of the functional fit to the measured displacement data and (b) the gage length used to estimate strain, this is part of an on-going research effort to quantify potential errors in the 3D measurement methodology.

After completing the alignment and calibration processes, image data was acquired as follows. First, prior to loading the specimen, a series of overlapping images of 4mm by 4mm areas located approximately 38 mm ahead of the initial

crack position were acquired as reference images for later strain measurements. The camera system was then translated to observe the initial crack tip region. During loading, images were acquired of the crack tip region. The system was translated and rotated during the experiment so that the crack tip area could continue to be imaged as the crack grew.

The three-dimensional surface displacement fields were converted to in-plane strain fields in the vicinity of the initial crack tip region using the Lagrangian strain formulation in terms of the displacement gradients

$$\varepsilon_{xx} = \partial u/\partial x + 1/2\{ (\partial u/\partial x)^2 + (\partial v/\partial x)^2 + (\partial w/\partial x)^2 \}$$
$$\varepsilon_{yy} = \partial v/\partial y + 1/2\{ (\partial u/\partial y)^2 + (\partial v/\partial y)^2 + (\partial w/\partial y)^2 \} \quad (5)$$
$$\varepsilon_{xy} = 1/2 \{ (\partial u/\partial y + \partial v/\partial x) + (\partial u/\partial x\, \partial u/\partial y + \partial v/\partial x\, \partial v/\partial y + \partial w/\partial x\, \partial w/\partial y) \}$$

Here, (u,v,w) are displacements relative to an (x,y,z) coordinate system located at the initial crack tip position. Since unknown rigid body deformations were introduced during the experiment by moving the optical setup, it is important to note that the strain tensor components defined by Eq. (5) are invariant with respect to arbitrary rigid body motion

To obtain the displacement gradient field, a local surface fit was obtained for each of the $u(x_i,y_i,z_i)$, $v(x_i,y_i,z_i)$ and $w(x_i,y_i,z_i)$ data sets and the partial derivatives of the resulting best-fit displacement surfaces were used in Equation (5) to determine the surface strains. To ensure optimal accuracy of the displacement gradients, two approaches were taken in the data analysis. First, a strip of data was removed from the region along the crack line and the data was processed as three separate regions to eliminate errors in the measurements that could be introduced if the subsets crossed the crack line. Second, data along the edges of each of the three separate regions were discarded to eliminate errors in the gradient data introduced by edge effects.

EXPERIMENTAL RESULTS

Using the procedures described in the previous sections, COD was measured throughout the crack extension process for all S_T/S_P values using Equations (2,3,4). Figure 4 presents the first known three-dimensional COD-Δa measurements from the tension-torsion tests, as well as a horizontal line representing the mean value for the COD data for $\Delta a > 10$ mm. In this work, all crack extension measurements are derived from the camera images using established procedures for identifying the growing crack tip location in each image *[1-3]*.

In addition to COD, the surface displacement fields were also measured during the loading process. For $S_T/S_P = 3.32$, typical results for the out of plane displacement field, (w(x,y)), just after initiation of crack extension are shown in Figure 5. Here, positive values for w(x,y) correspond to motion towards the camera.